J Solid State Electrochem (2003) 7: 271–276
DOI 10.1007/s10008-002-0336-x

ORIGINAL PAPER

M. Miranda-Hernández · J.A. Ayala
Marina E. Rincón

Effect of surface structure on the charge storage capacity of carbon black electrodes

Received: 6 June 2002 / Accepted: 9 October 2002 / Published online: 12 November 2002

Abstract In this work we study the effect of surface structure on the charge storage capacity of carbon black electrodes with various changes in surface chemistry, morphology, and doping species. Cyclic voltammetry and chronopotentiometry studies, performed under alkaline conditions with carbon paste electrodes, indicate the importance of surface structure and grain size on the faradic and capacitive charge contributions of these materials. Among the various carbon blacks studied, the lithiated material shows superior charge storage capacity, suggesting the importance of alkaline metals and oxygenated groups on the carbon surface. For the graphitic carbon, the appearance of a reversible redox process with cycling resembles the electrochemical behavior reported for hydrogen storage in carbon nanotubes.

Keywords Electrochemical capacitor · Carbon black · Carbon paste

Introduction

The development of new materials for use as electrochemical capacitors is of great scientific and technological interest [1, 2]. The aim is to develop new types of accumulators with specific power larger than 10 kW/kg and enhanced durability (superior to 10^6 cycles). The principal advantage of the new storage devices is their capacity for dynamic propagation of charge, which can be used in many hybrid power sources, electrical vehicles, etc. Currently, electrochemical accumulators do not satisfy the demands of power and durability, owing to the inherent limitations of the physicochemical processes. This is that electrochemical reactions are needed for charges to be stored or released, implying electron charge transfer through the electrode interface and changes in the oxidation state of the constituent materials. In contrast to electrochemical accumulators, in electrochemical capacitors, charge storage occurs mainly in the double layer, through electrostatic forces and without the need for phase transformations in the electrode material. When both processes take place (i.e., electrostatic storage accompanied and enhanced by faradic processes) the device is a pseudocapacitor.

Various materials have been characterized as electrochemical capacitors [3, 4, 5, 6, 7, 8, 9], in aqueous an non-aqueous electrolytes [10, 11, 12, 13], and the limitations of large resistivity in non-aqueous media, or the limited potential window and corrosion problems of aqueous electrolytes, have been thoroughly highlighted. New allotropic forms of carbon (C_{60} and nanotubes) have been proposed as an alternative for materials that corrode in aqueous media [14, 15, 16]. Unfortunately, the high cost of fullerenes does not allow their application as large-area electrochemical capacitors. Consequently, most of the development on new materials for electrochemical capacitors is based on carbon [8, 17, 18, 19, 20, 21, 22]. The strong dependency of the physicochemical properties of these materials with their route of synthesis, and the effect of surface structure on the irreversible/reversible capacity of various graphitic carbon electrodes, maintains interest in the performance of modified carbons. As an example, irreversible capacity has been associated with film formation and found to be proportional to the surface area in low structured carbon [23]. In carbons with high structure and low surface area, this proportionality does not hold. In these materials the different reactivity of basal and edge planes plus the high anisotropy of graphitic carbon (when compared

Presented at the XVII Congress of the Mexican Electrochemical Society, 26–31 May 2002, Monterrey, Mexico

M. Miranda-Hernández · M.E. Rincón (✉)
Centro de Investigación en Energía-UNAM,
Apartado Postal 34, Temixco, Morelos 62580, Mexico
E-mail: merg@cie.unam.mx
Tel.: +52-555-6229748

J.A. Ayala
Columbian Chemicals Co.,
1800 West Oak Commons Ct., Marietta, GA 30062, USA

to polycrystalline carbon) have been suggested to play a dominant role. In other words, irreversible capacity could come from the exfoliation process, which does not depend on surface area and is rarer in randomly oriented crystalline domains than in uniformly aligned ones. In the latter, a microfracture can propagate easily throughout the solid [23].

In this work, various types of carbon black were analyzed by cyclic voltammetry and chronopotentiometry techniques in alkaline media (6 M KOH). The stability of the materials to positive and negative current pulses of various magnitude, the evaluation of charge storage and release, and the capacitive or pseudocapacitive behavior of the current-potential curves will be correlated with the surface structure, surface area, particle size and composition of the various materials. Other possible applications of the carbon blacks will be discussed.

Experimental

Electrochemical measurements were carried out with Basic Autolab W/PGSTAT30&FRA equipment, in a conventional three-electrode cell consisting of a working carbon paste electrode, a graphite counter electrode, and a Hg/HgO/1 M KOH reference electrode (+0.2 V vs. NHE). The aqueous electrolyte was 6 M KOH and both reference and counter electrodes were kept in separate compartments. Carbon blacks supplied by Columbian Chemical Co. from three different experimental trials were characterized: C-SMT, C-LIMT, and C-MA21. Table 1 presents some of the characteristics of these carbon blacks. The major difference between the C-SMT and the C-LIMT is that the latter has been doped with lithium and has a very low sulfur content. Carbon paste electrodes were prepared by mixing carbon black (CB) and silicon oil (S) with a weight ratio of CB:S = 80:20, except for the material labeled C-MA21 where an inverted weight ratio of 20:80 was required owing to its significantly higher surface area and structure. However, the viscosity (consistency) of the paste was equivalent in all electrodes. A CB:S = 20:80 ratio could not be used in C-SMT and C-LIMT because the paste became too liquid and did not hold to any surface.

Once the consistency of the paste was right, it was supported in a 0.4-mm thickness Teflon ring (0.96 cm^2) with stainless steel as the back contact. All the experiments took place under stationary conditions, with nitrogen being bubbled through the electrolyte prior to (30 min) and between all measurements. Moreover, the nitrogen was kept flowing over the solution during the measurements. In each case, and particularly for C-MA21 where the low CB/S ratio could compromise the percolation mechanism required for electronic conduction, the bulk resistivity of the paste was monitored qualitatively against the ferro/ferricyanide reaction. To do this, cyclic voltammograms for 0.01 M ferro/ferricyanide/1 M KCl were obtained in the potential range of ± 1 V vs. the saturated calomel electrode. Regardless of different CB/S ratios, all carbon paste electrodes reproduce reasonable well the typical electrochemical response of this redox couple (i.e., the area under the peaks is similar and symmetric, while the observed peak currents deviate by a maximum of 20 mV). Additionally, to ensure similar interfacial conditions and good reproducibility, each experiment was run with a renewed surface.

Cyclic voltammetry studies in alkaline media were performed in the potential range of 0.4 to –1.6 V vs. Hg/HgO/1 M KOH. The sweep was initiated at the rest potential (V_r) in the negative direction and with a scan rate of 10 mV/s. For some experiments the material was polarized at –1.6 V vs. Hg/HgO/1 M KOH for a specific time, followed by a linear potential scan in the positive direction. A constant double current pulse (±) was used for the chronopotentiometry studies, and their magnitude depended on the type of carbon black.

Results and discussion

Figure 1 shows the cyclic voltammogram of the 10th (last) cycle for the various carbon blacks. The current associated with C-SMT and C-LIMT is very similar, typical of an electrochemical pseudocapacitor, with dominant electrostatic charging and minor contributions due to faradic processes. In contrast, the capacitive charge of C-MA21 is minimal and there is a strong contribution of a fast electrochemical reaction at –1.1 V vs. Hg/HgO. In general, the electrochemical behavior of C-MA21 is different to the other carbon blacks. For example, it has a low current response in the potential interval analyzed, and superior overpotential for water electrolysis. The studies done on ferro/ferricyanide, where all the electrodes gave similar responses, suggest that the inverted CB/S ratio of C-MA21 is not the reason for its different electrochemical behavior.

The charge/discharge response of the various carbon blacks as a function of the number of cycles is given in Fig. 2 under variable and constant currents. The potential-time curves of the chronopotentiometry studies were converted into potential-charge diagrams, and normalized according to the weight of carbon. In Fig. 2a the perturbation consisted of 100 s cathodic pulses starting at -3×10^{-5} A (first cycle) and ending at -7×10^{-5} A (fifth cycle). The 200 s anodic pulse was 2×10^{-5} A in each cycle. Chronopotentiometry curves with pulses of $\pm 6\times10^{-5}$ A for C-LIMT and $\pm 1.5\times10^{-4}$ A for C-MA21 are shown in Fig. 2b and c, respectively. In these figures the width of the pulse was different in the cathodic (direct) and anodic (inverse) directions. Figure 2b is the result of 50 s/100 s direct/inverse pulses, while Fig. 2c corresponds to 100 s/200 s direct/inverse pulses. Curves obtained for C-SMT are not shown since they are similar to the ones presented for C-LIMT.

Table 1 Morphology parameters and chemical composition of carbon blacks

Sample	Mean particle size (nm)	BET surface area (m^2/g)	DBPA[a] (mL/100 g)	Sulfur (%)	Lithium (ppm)
C-SMT	390	6.6	42	0.35	< 1
C-LIMT	390	5.5	42	0.02	700
C-MA21	25	80	170	0.01	–

[a]Dibutyl phthalate absorption

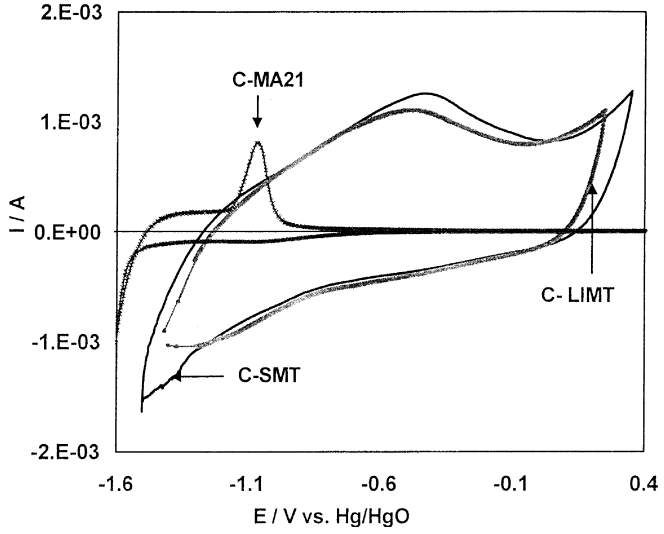

Fig. 1 Cyclic voltammograms (10th cycle) in 6 M KOH for carbon paste electrodes based on different carbon blacks. The potential swept (10 mV/s) starts at the rest potential in the negative direction. The electrode geometric area was 0.96 cm^2 and the paste had a carbon content of 0.1122 g

Chronopotentiometry studies at $\pm 1.5\times10^{-4}$ A could not be sustained for a long time (more than five cycles) for both C-SMT and C-LIMT because the evolution of hydrogen compromised the integrity of the paste.

Under a variable cathodic current (Fig. 2a) there is a shift of C-LIMT to more negative potentials as the intensity of the cathodic pulse increases. Moreover, the complexity of the curves also increases with current intensity. The various inflexions on the potential-capacity curves correspond to transitions from one electrochemical reaction to another. Therefore, as the cathodic current increases, two electrochemical reactions appear at –0.4 V and –1 V vs. Hg/HgO. The last event is expected to be related to hydrogen adsorption and intercalation. Additionally, when C-LIMT is subjected to equal perturbation currents of 60 μA, the process at –0.4 V vs. Hg/HgO takes over the hydrogen adsorption/intercalation reaction (Fig. 2b). For C-MA21, several electrochemical processes are observed in the potential-capacity curves owing to the higher current intensity of the pulses. In contrast to C-LIMT, in this carbon black the electrochemical reaction at –1 V vs. Hg/HgO becomes dominant as the number of cycles increases.

The materials compared in Fig. 2, C-LIMT and C-MA21, have surface areas of 5.5 m^2/g and 80 m^2/g, respectively. More important, the particle size of C-MA21 is substantially smaller than the other carbons

►

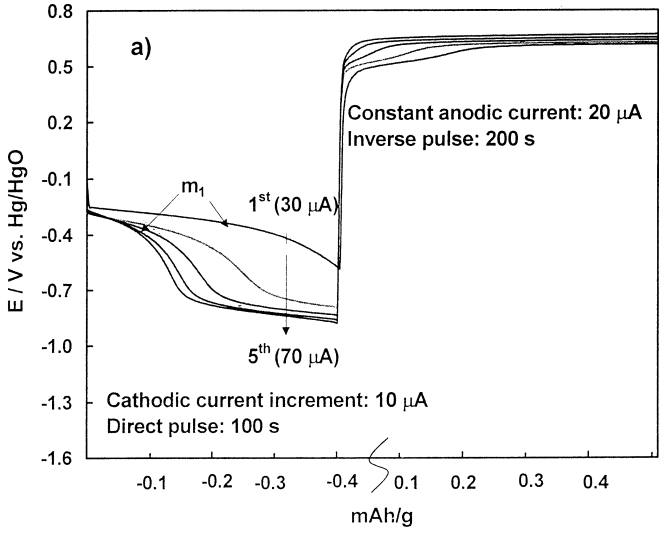

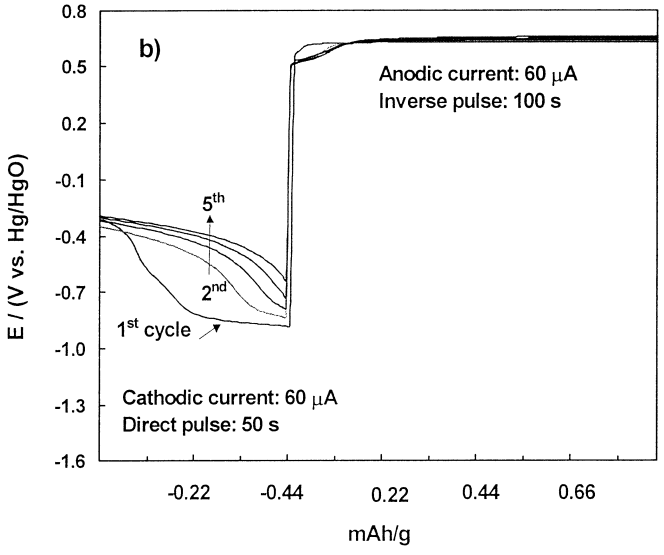

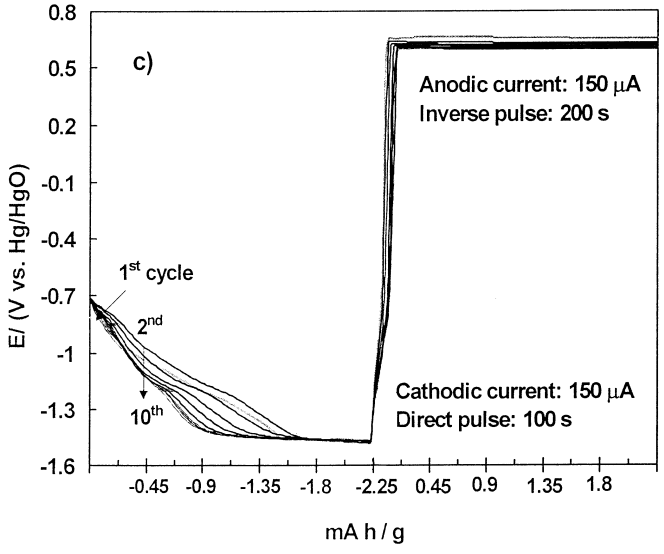

Fig. 2 Chronopotentiometry curves in 6 M KOH for: **a** C-LIMT under a variable cathodic pulse (30–70 μA/100 s) and constant anodic pulse (20 μA/200 s); **b** C-LIMT under a constant double current pulse of ± 60 μA or $\pm 2.7\times10^{-4}$ A/g (cathodic pulse/50 s, anodic pulse/100 s); **c** CMA21 under a constant double current pulse of ± 150 μA or $\pm 1.3\times10^{-3}$ A/g (cathodic pulse/100 s, anodic pulse/200 s)

studied, as evidenced in Table 1. In addition, C-MA21 has been submitted to a thermal treatment of 2200 °C in an inert atmosphere and Fig. 3 clearly demonstrates that a partial graphitization process has occurred for this carbon black. That is, long parallel layering is observed for the C-MA21 versus the typical disoriented turbostatic layer morphology of C-SMT and C-LIMT, also shown in Fig. 3. The abundance of oxygen-containing groups in the carbon surface is much more important for C-LIMT and C-MST than for C-MA21, since the latter loses almost all oxygen functionality due to the partial graphitization process of the thermal treatment.

The correlation between different morphologies and cathodic behavior of the various carbon blacks is clearer in the density of states (DoS) representation. Figure 4 shows the curve of dQ/dV vs. V, where Q represents the

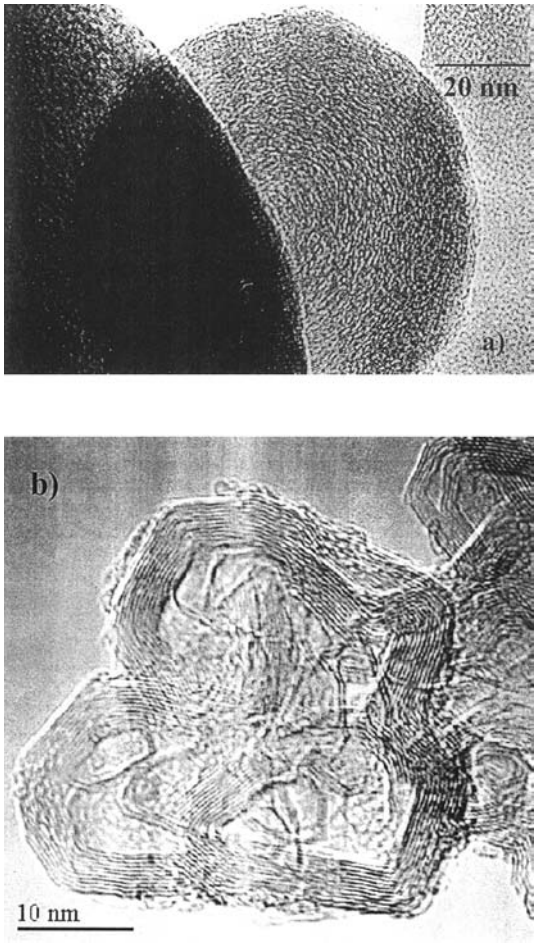

Fig. 3 TEM micrographs of **a** C-LIMT and **b** C-MA21. Lamella arrangement can be seen near the surface for C-MA21

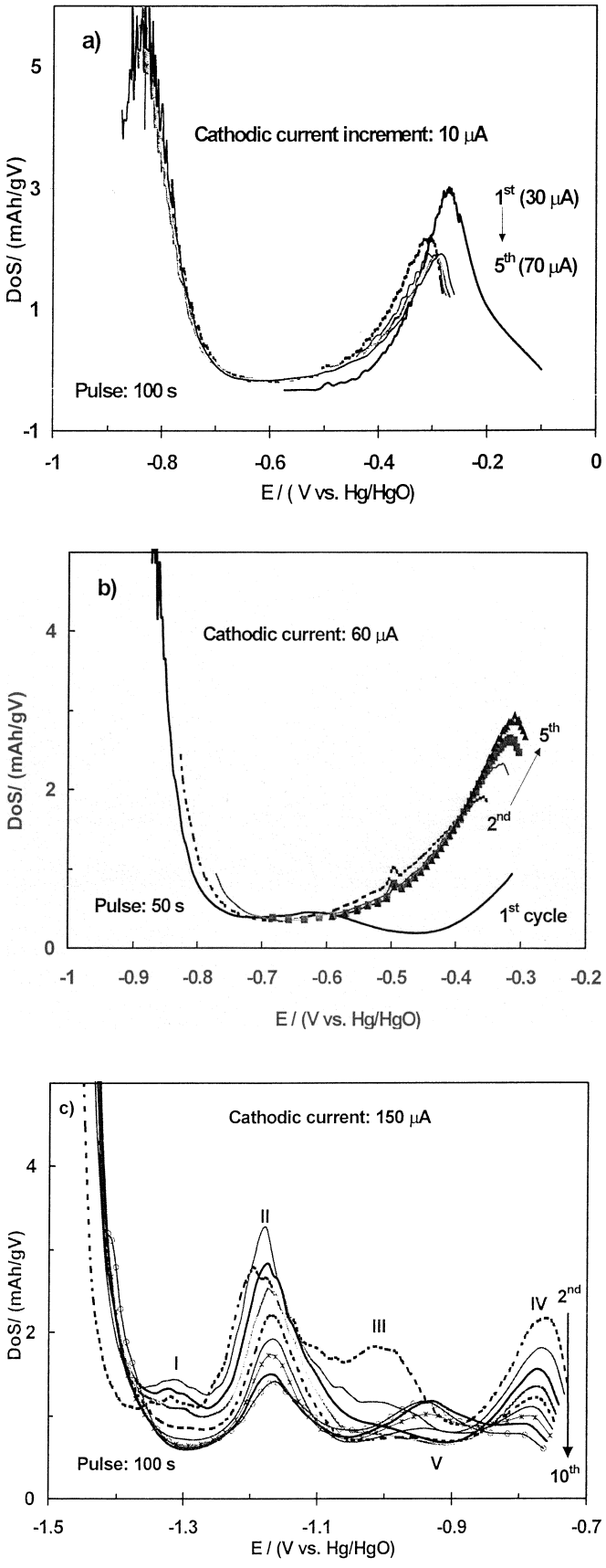

Fig. 4 Density of states for electroactive species as a function of the equilibrium potential: **a** C-LIMT under a variable perturbation current; **b** C-LIMT under a constant perturbation current; **c** C-MA21 under constant perturbation current. Details in legend to Fig. 2

charge per unit mass. As expected, the representation corresponding to the variable current pulse (Fig. 4a) shows the two electrochemical processes that were evident in the curves of C-LIMT after the first cycle. Without considering the first pulse, the potential spread of the peaks is relatively small during cycling. On the other hand, under a constant perturbation of 60 μA the DoS representation of this carbon black (Fig. 4b) indicates that cycling facilitates both cathodic processes since the peaks move to less negative potentials as the number of cycles increases, and the charge imposed accumulates in the event occurring at –0.4/–0.3 V vs. Hg/HgO. In high contrast to C-LIMT and C-SMT, Fig. 4c shows the larger complexity of the C-MA21 carbon black curves obtained under a stronger perturbation pulse (150 μA). A minimum of four processes take place in C-MA21 and their magnitude decreases with the number of cycles (zones I, II, III and IV, with approximate values of –1.3, –1.18, –1.0 and −0.78 V vs. Hg/HgO, respectively). In addition, another process appears during cycling (zone V at –0.95 V vs. Hg/HgO). There appears to be a correspondence of process V with the anodic peak at –1.1 V vs. Hg/HgO observed in the cyclic voltammogram of this material. The rich electrochemical behavior of C-MA21 cannot be explained in terms of its poor surface chemistry and reflects the large anisotropy expected for a graphitic carbon. That is, adsorption/intercalation of hydrogen and/or other electroactive species can be occurring in basal or edge surfaces with different degrees of curvature. The nature of zone V and the anodic peak at –1.1 V vs. Hg/HgO are not clear. The fact that these events appear during cycling could hint that they may be related to exfoliation or corrosion of graphene layers and/or that the electrochemical active species is in the bulk of the solution, since the redox processes of surface groups are expected to disappear with cycling. More studies will be directed to identify the nature of this electrochemical reaction, whose large reversibility resembles the behavior found in the electrochemical storage of hydrogen in carbon nanotubes [24, 25].

The highly disordered and low structured nature of C-LIMT helps with the fast stabilization of the capacitive current of this material. Regardless of its low surface area, C-LIMT has a higher DoS (larger capacity) than the graphitic carbon black (area under the peaks that grow or remain constant with number of cycles), but it is limited by its smaller potential window. On the other hand, most of the surface area of C-MA21 is not electrochemically active, but this material has a larger overpotential for water electrolysis. Still, the nature of the process at –1.1/-0.95 V vs. Hg/HgO must be clearly resolved.

Table 2 gives the response of the various materials after they were polarized at –1.6 V vs. Hg/HgO. The potential window of –1.6 to 0.4 V is insufficient to recover all the charge applied to C-MA21, but it is too large for C-SMT since, at –1.6 V vs. Hg/HgO, irreversible hydrogen evolution occurs in this carbon black.

Table 2 Relation of charge applied/recovered from carbon blacks submitted to cathodic polarization (–1.6 V vs. Hg/HgO) during various times followed by an anodic potential sweep at 10 mV/s

	t (s)	Q_i (mC/m^2)[a]	Q_a (mC/m^2)	Q_a/Q_i (%)
C-MA21	90	0.80	0.012	1.5
	300	1.38	0.001	0.1
	1200	1.17	0.059	5.0
C-LIMT	90	11.76	3.97	33.7
	300	55.48	23.48	42.3
	600	69.52	52.45	75.4
	1200	56.68	41.80	73.7
C-SMT	90	11.27	0.41	3.6
	300	44.25	1.47	3.3
	600	435.83	18.77	4.3
	1200	1802.14	56.33	3.1

[a] Q_i: charge accumulated during the initial polarization. Q_a: charge integrated during the anodic potential sweep

However, this potential window (–1.6 to 0.4 V) seems to be just right for C-LIMT, which recovers almost 70% of the charge at the largest polarization time. The different behavior of C-SMT and C-LIMT is more related to the different chemical compositions of these carbon blacks than to their different morphologies. The presence of lithium in C-LIMT seems to provide stronger adsorption sites relative to the undoped C-SMT carbon black, increasing the overpotential for hydrogen evolution.

Conclusions

In this work we report the electrochemical behavior of carbon blacks with different surface structures, surface chemistries and morphologies. The influence of these variables on the chronopotentiometry curves was discussed. The disordered nature and lower structure of C-LIMT helps to increase the magnitude and kinetics of the electrostatic adsorption/desorption processes, even though no reversible faradic processes were observed in this carbon black. On the other hand, the large overpotential of the graphitic carbon C-MA21 is manifested in the experimental results, and may be attributed to the large anisotropy of its reactive sites. In this carbon, the fast redox process at around –1 V vs. Hg/HgO resembles the electrochemical hydrogen storage behavior observed in carbon nanotubes.

Acknowledgements The authors are grateful to the Electrochemical Laboratory of UAM-Iztapalapa (México) for assistance with the electrochemical characterization of the materials, to the Columbian Chemicals Company for the materials supplied, and to CONACyT-MEXICO for financial support.

References

1. Conway BE (1991) J Electrochem Soc 138:1539
2. Sarangapani S, Tilak BV, Chen CP (1996) J Electrochem Soc 143:3791
3. Ardizzone S, Fregonara G, Trasatti S (1990) Electrochim Acta 35:263

4. Kötz R, Stucki S (1986) Electrochim Acta 31:1311
5. Zheng JP, Cygan PJ, Jow TR (1995) J Electrochem Soc 142:2699
6. Arbizzani C, Mastragostino M, Meneghello L (1996) Electrochim Acta 41:21
7. Momma T, Liu X, Osaka T, Ushio Y, Sawada Y (1996) J Power Sources 60:249
8. Frackowiak E, Béguin F (2001) Carbon 39:937
9. Teng H, Chang YJ, Hsieh CT (2001) Carbon 39:1981
10. Ue M, Ida K, Mori S (1994) J Electrochem Soc 141:2989
11. Kivi Y, Saito T, Kurata M, Tabuchi J, Ochi A (1996) J Power Sources 60:219
12. Zheng JP, Jow TR (1997) J Electrochem Soc 144:2417
13. Ingram MD, Pappin AJ, Delalande F, Poupard D, Terzulli G (1998) Electrochim Acta 43:273
14. Guangli C, Brindra L, Fisher ER, Martin CR (1998) Nature 393:346
15. Liu CY, Bard AJ, Wudl F, Weitz I, Heath JR (1999) Electrochem Solid State Lett 2:577
16. Honda K, Rao TN, Tryk DA, Fujishima A, Watanabe M, Yasui K, Masuda H (2001) J Electrochem Soc 148:A668
17. Ishikawa M, Sakamot A, Morita M, Matsuda Y (1996) J Power Sources 60:233
18. Miller JM, Dunn B (1999) Langmuir 15:799
19. Miller JM, Dunn B, Tran TD, Pécala RW (1997) J Electrochem Soc 144:L309
20. Osaka T, Liu X, Nojima M, Momma T (1999) J Electrochem Soc 146:1724
21. Shi H (1996) Electrochim Acta 41:1633
22. Qu D, Shi H (1998) J Power Sources 74:99
23. Chung GC, Jun SH, Lee KY, Kim MH (1999) J Electrochem Soc 146:1664
24. Lee SM, Park KS, Choi YC, Park YS, Bok JM, Bae DJ, Nahm KS, Choi YG, Yu SC, Kim N, Frauenheim T, Lee YH (2000) Synth Met 113:209
25. Rajalakshmi N, Dhathathreyan KS, Govindaraj A, Satishkumar BC (2000) Electrochim Acta 45:4511